

# Study on the Impact of Silicon Doping Level on the Trench Profile Using Metal-Assisted Chemical Etching

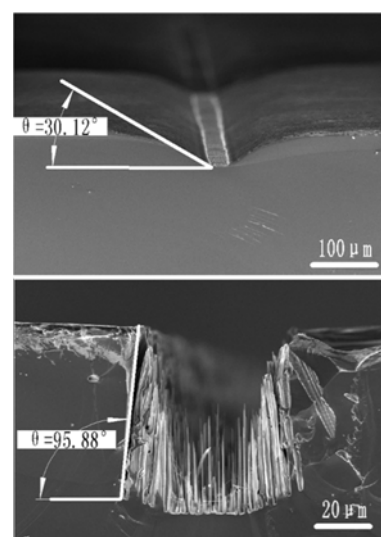
Zhe Cao, Qiyu Huang,\* Chuanrui Zhao, and Qing Zhang

Department of Micro/Nano-electronics, Shanghai Jiao Tong University, Shanghai, 200240, China

(received date: 22 June 2016 / accepted date: 18 August 2016 / published date: 10 November 2016)

Metal-assisted chemical etching (MACE) has been used as a promising alternative method to fabricate micro/nano-structures on silicon substrates inexpensively. In this paper, profiles of deep trenches on silicon substrates, with different doping levels, fabricated by MACE were studied. A layer of interconnected gold islands was first deposited onto the silicon substrate as catalyst. Electrochemical etching was then performed in a hydrofluoric acid (HF) and hydrogen peroxide (H<sub>2</sub>O<sub>2</sub>) mixture solution with different HF-to-H<sub>2</sub>O<sub>2</sub> ratio  $\rho$  ( $\rho = [\text{HF}]/([\text{HF}] + [\text{H}_2\text{O}_2])$ ). Vertical deep trenches were fabricated successfully by using this method. It was observed that even under identical experimental condition, sidewalls with various tilting angles and different morphology could still form on silicon substrates with different resistivity. This possibly because with different resistivity silicon substrate, the gradient of holes in it greatly changed, and so did the final morphology. As a result, the tilting angle of etched trench sidewall can be tuned from 6° to 96° using silicon substrates with different resistivity and etchants with different  $\rho$ . By applying the angle-tuning technique revealed in this study, high aspect ratio patterns with vertical sidewalls could be fabricated and three-dimensional complex structures could be designed and realized in the future.

**Keywords:** metal-assisted chemical etching, deep trenches, anisotropic etching, silicon doping level, profile control



## 1. INTRODUCTION

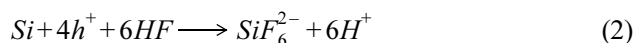
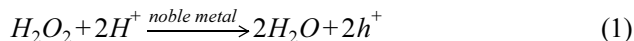
High aspect ratio vertical structures on a silicon substrate have been found extensive applications, such as Micro-Electro-Mechanical Systems (MEMS),<sup>[1]</sup> photovoltaic cells,<sup>[2,3]</sup> biomedical sensors,<sup>[4,5]</sup> high energy density batteries,<sup>[6]</sup> thermoelectric modules,<sup>[7]</sup> and X-ray lenses.<sup>[8]</sup> There are two main methods to fabricate the vertical trenches, dry etching and wet etching. The dry-etching methods include reactive ion etching (RIE),<sup>[9]</sup> inductive coupled plasma (ICP)-RIE, and chemical assisted ion beam etching (CAIBE). However, the necessary instruments are usually expensive. Even though wet-etching methods like traditional chemical etching<sup>[10]</sup> and acidic electrochemical etching,<sup>[11-13]</sup> on the

contrary, are much cheaper, traditional chemical etching with base can only generate grooves on (110) oriented Si substrates. As for the acidic electrochemical etching, it happens laterally and vertically simultaneously, which makes it challenging to create high aspect ratio features. Therefore, a new etching method is highly demanded to overcome the limitations of both dry etching and the traditional wet etching.

In previous studies, metal assisted chemical etching (MACE) has been demonstrated as a promising low-cost alternative to fabricate the micro/nano-structures on silicon substrates.<sup>[14,15]</sup> When performing MACE, a thin layer of noble metal is deposited onto a silicon substrate as the catalyst, by using either physical vapor deposition (PVD) or chemical reaction. The noble metal that can be used as catalyst for the etching include Ag, Au, Pt, and *et al.*<sup>[16]</sup> Si substrates with catalyst is immersed into an etchant solution

\*Corresponding author: qiyu@sjtu.edu.cn  
©KIM and Springer

containing  $\text{H}_2\text{O}_2$  and HF afterwards.  $\text{H}_2\text{O}_2$  is catalytically decomposed on the metal-liquid interface and the holes ( $\text{h}^+$ ) are generated, as indicated in Eq. (1). The holes participate in the dissolving of Si, which occurs at the Si-Au interface as expressed in Eq. (2).



Because the etch rate where the catalyst is presented is much faster, the noble metal ions move into the etched space and catalyze the reaction further, which makes the etching anisotropic. Ideally, the morphology of the etched silicon substrate will be exactly the same as the noble metal pattern deposited on it.

MACE has been widely used in the fabrication of silicon nanowires (SNW) and macroporous silicon.<sup>[17,18]</sup> It consists of two mechanisms: the mass-transport (MT) and the charge-transport (CT).<sup>[15]</sup> MT is the transport of etchant (e.g.  $\text{H}_2\text{O}_2$ , HF and  $\text{h}^+$ ) and products (e.g.  $\text{SiF}_6^{2-}$  and  $\text{H}_2\text{O}$ ). The noble metal deposited on the silicon substrate needs to be porous, so that the mass can pass through the intervals among the interconnected metal islands.<sup>[19]</sup> Otherwise, the etching will happen only at the edge of the metal layer resulting in a shallow and uneven trench.<sup>[14]</sup> There are many factors that influence the charge transport, such as the doping level of the Si substrate and the concentration of the etchant. These factors influence the etching rate and the final morphology of the substrate through charge transport process.<sup>[20,21]</sup>

Many theories on the mechanism of the mass transport of etchant and silicon substrate during MACE by using a thin layer of Au as catalyst have been proposed. These include the transport of silicon ions through the pores in Au layer or by diffusion underneath the Au layer.<sup>[22]</sup> When the deposited Au layer is thick and no more pores exist, reactant and products will no longer be able to transfer through the Au layer. Lateral mass transport will happen at the Au edge instead, which was demonstrated by Li *et al.*<sup>[15]</sup> To avoid the lateral mass transfer happening, the thickness of the metal layer should be limited strictly. Lajvardi *et al.*<sup>[19]</sup> compared the catalyzed etching with Au layer of the thicknesses of 3 nm, 6 nm and 10 nm respectively when fabricating Si nanowires. The pores of the layer decreased together with increase of the thickness. In order to form Si nanowires, the optimum thickness of Au was determined to be 6 nm. The etch rate had no obvious relation to the size of pores or spacing among the interconnected islands in the Au layer. When deciding the thickness of the catalyst layer in this work, it is important that the pores in the Au layer are neither too big to ensure the MACE have a reasonably good resolution nor too small to allow the materials pass through.

Therefore, a 10 nm Au layer is selected for this study.

In the few previous literature that was about the trench etching, most were focused on the influence of type<sup>[19]</sup> and thickness<sup>[17]</sup> of the metal deposited on the silicon substrate or the concentration of the etchant.<sup>[20]</sup> Our study is based on previous work and investigates the impact of different doping levels of the wafer on the etched morphology. This might give some insights to the etching mechanism. Etchants with different  $\rho$  (we define  $\rho = [\text{HF}] / ([\text{HF}] + [\text{H}_2\text{O}_2])$ ) value were also investigated in this paper.

## 2. EXPERIMENTAL PROCEDURE

*P*-type, Boron-doped, (100) oriented, and polished silicon wafers with different doping levels were used in our study. Their resistivity ranged from 0.005  $\Omega\cdot\text{cm}$  to 10  $\Omega\cdot\text{cm}$ . A standard RCA cleaning sequence was used to clean the wafers (85 °C 1:1:5  $\text{NH}_4\text{OH}:\text{H}_2\text{O}_2:\text{H}_2\text{O}$  solution for 10 min; deionized water (DIW) rinse; 1:10 HF: $\text{H}_2\text{O}$  for 1 min; DIW rinse; 85 °C 1:1:6 HCl: $\text{H}_2\text{O}_2:\text{H}_2\text{O}$  solution for 10 min; DIW rinse). After being cleaned thoroughly with running DIW, the wafers were fully dried with  $\text{N}_2$  flow.

The simplified fabrication steps are illustrated in Fig. 1. A 2  $\mu\text{m}$  thick photoresist (SUN-lift 130) film was first spin-coated on the silicon wafers and exposed with a UV mask aligner (URE-2000/35). After baked on a hotplate at 110 °C for 90s, the wafers were further developed in 2.38% TMAH developer at room temperature for 20 s. The patterns consisted of lines, squares, rectangles and circles in the size range of 50-200  $\mu\text{m}$ , which were designed to test the resolution of the MACE method. The wafers with patterned resist underwent an oxygen plasma bombardment (performed in a Harrick Plasma RIE system operating at a pressure of 800 mTorr and 20 W of power for 3 min) to render the

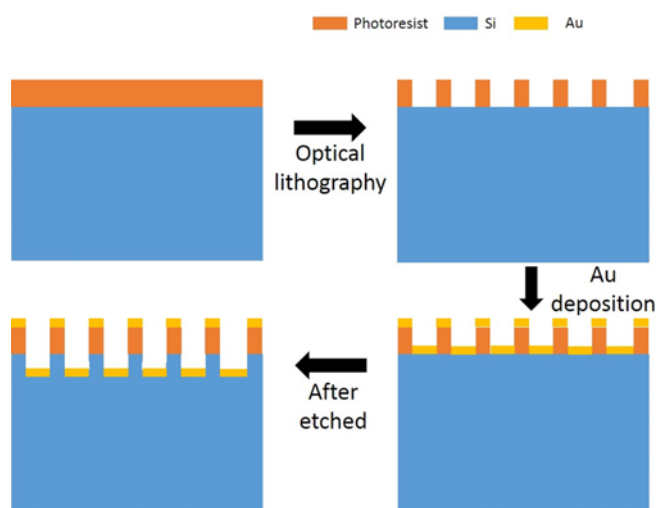


Fig. 1. The fabrication of trenches on a Si substrate by MACE.

exposed silicon surface oxygen-terminated (Si-O). A 10 nm thick Au catalyst layer was evaporated using a Denton Multi-Pocket e-beam evaporator at a rate of  $1 \text{ \AA}/\text{sec}$  in a chamber with the vacuum of  $6.7 \times 10^{-6}$  Torr. The thickness of Au layer was measured by a built-in monitor.

Etchant  $\rho(0.25)$  (representing  $\rho = 0.25$ ) was prepared by mixing 2.97 M HF and 8.52 M  $\text{H}_2\text{O}_2$ . While the etchant  $\rho(0.37)$  was obtained by mixing 3.96 M HF and 6.71 M  $\text{H}_2\text{O}_2$ . The etching was conducted by gently immersing the sample in the etchant in a sealed polyethylene container for 1 hour. The etchant was agitated with a magnetic stirring bar considering not being able to refresh the etchant frequently due to the elaborate structures on the silicon substrates. After the MACE was completed, the samples were ultrasonically cleaned in acetone for 3 min to remove the photoresist and the gold layer on top. Scanning electron microscope (SEM) images were taken by Zeiss Ultra Plus field emission (TFE) SEM, operating at 5 KV and a working distance between 8

and 15 mm, with an inserted Oxford EDS system.

### 3. RESULTS AND DISCUSSION

Figure 2 shows cross-sectional SEM images of the  $50 \mu\text{m}$  wide trenches on silicon wafers of different doping levels using  $\rho(0.25)$  and  $\rho(0.37)$  solutions respectively for 1 hour. These trenches are fabricated under identical conditions except  $\rho$ . We define the angle between horizon and the sidewall to be the tilting angle of a trench herein, as indicated in Fig. 2. The tilting angle of the trenches varies with the doping level of the Si substrates. With the increase of the resistivity of a wafer, which means a decrease for the doping level, the tilting angle of the etched trenches increases. Tilting angle and depth of the etched trenches on Si substrates of different resistivity are shown in Table 1. Please note that there are many ‘grass-like’ silicon nanowires exist on the bottom of the trench on the  $10.2 \Omega\cdot\text{cm}$  Si substrate, as

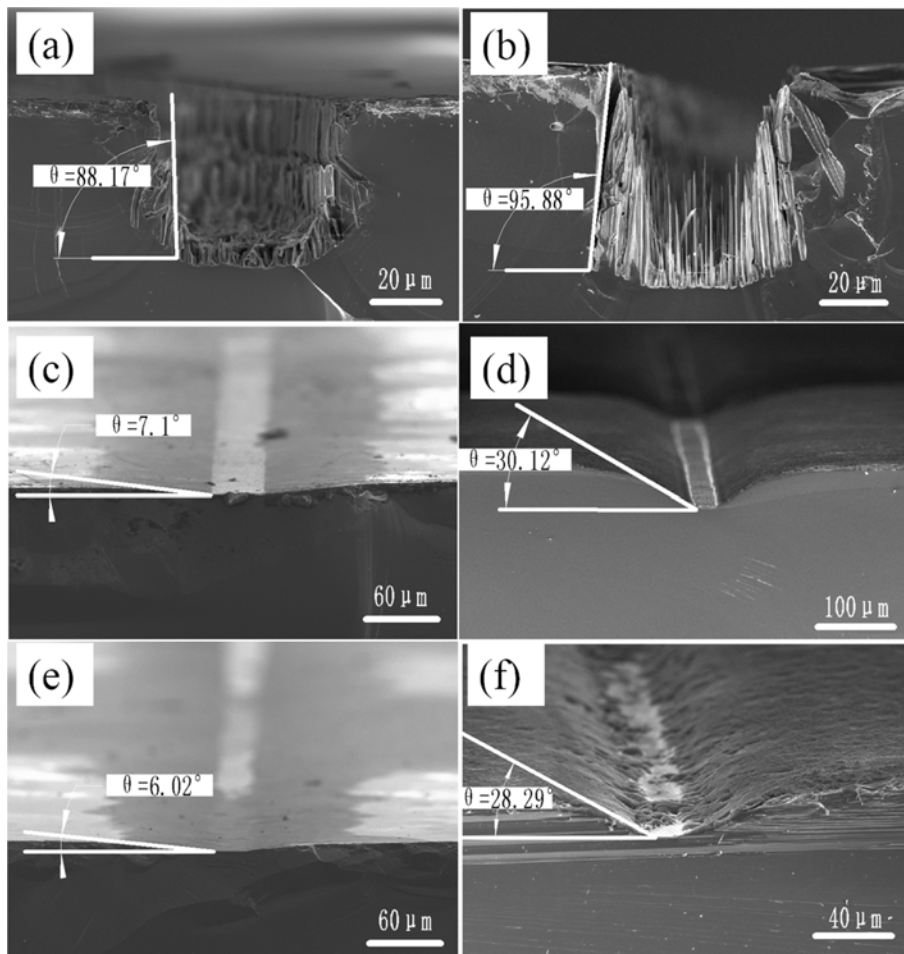


**Fig. 2.** Cross-sectional SEM images of silicon substrates of different resistivity with a 10 nm thick Au layer as the catalyst etched in a mixed etchant for 1 hour. (a)  $10.2 \Omega\cdot\text{cm}$  Si substrate and  $\rho(0.25)$  etchant; (b)  $10.2 \Omega\cdot\text{cm}$  Si substrate and  $\rho(0.37)$  etchant; (c)  $0.01 \Omega\cdot\text{cm}$  Si substrate and  $\rho(0.25)$  etchant; (d)  $0.01 \Omega\cdot\text{cm}$  Si substrate and  $\rho(0.37)$  etchant; (e)  $0.005 \Omega\cdot\text{cm}$  Si substrate and  $\rho(0.25)$  etchant; (f)  $0.005 \Omega\cdot\text{cm}$  Si substrate and  $\rho(0.37)$  etchant. All silicon substrates were P-type, (100) oriented and Boron-doped.

**Table 1.** Tilting angle and depth of the etched trenches on Si substrates of different resistivity.

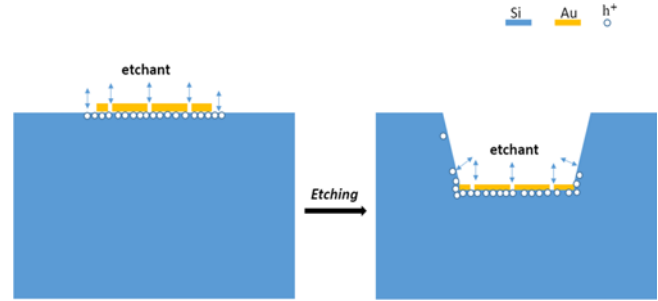
$\rho$	Resistivity ( $\Omega \cdot \text{cm}$ )	Tilting angle ( $^\circ$ )	Depth ( $\mu\text{m}$ )
0.25	10.2	$88 \pm 1$	48.4
	0.01	$7 \pm 0.5$	8.76
	0.005	$6 \pm 0.5$	7.26
0.37	10.2	$95 \pm 1$	70.76
	0.01	$30 \pm 1$	58.49
	0.005	$28 \pm 0.5$	27.94

cannot be seen in other highly-doped substrates. Figures 2(a), (c), and (e) show a gradual decrease of both the tilting angle and the trench depth with the decrease of the substrate resistivity for  $\rho(0.25)$  etchant. For an etchant with different  $\rho$ , like 0.37, the similar phenomena could be observed, as displayed in Figs. 2(b), (d), and (f).

We hypothesize that for a specific  $\rho$ , the key parameter controlling the tilting angle is the hole concentration of the substrate. There are two sources of holes that involved in the reaction. One is generated by  $\text{H}_2\text{O}_2$  in the etchant at the noble metal-silicon interface, in the form of freely available holes. The other is from the Si substrate itself, trapped inside silicon. However, under the catalysis of noble metals, the trapped holes can be released and join the reaction. Only when the concentration of the holes provided by these two sources is consistent with the concentration of HF, vertical etching can be happened. Zhang *et al.*<sup>[18]</sup> found that with the increase of doping level, the Si nanowires they obtained by MACE became rougher, some of which contained micro- or mesopores. This showed that the silicon substrate had an impact on the formation of Si nanowires by providing holes, and the amount of the holes was related to the substrate doping level.

For a highly doped *P*-type Si substrate, the holes are relatively abundant. Due to less band bending at the highly doped Si/solution interface compared to the lightly doped, more holes are available for diffusion to Si regions where having no catalyst.<sup>[21]</sup> According to Eq. (2), Si is dissolved by HF as long as there are surplus holes existed. As a result, the etching happens both laterally and vertically, in other words, it becomes quasi-isotropic etching. Moreover, because of the existence of abundant holes, no randomly aligned ‘grasses’ are observed in the trench.

When the doping level decreases, the concentration of holes is reduced correspondingly. The HF is, on the other hand, relatively plentiful. Once holes are generated at the Si/noble metal interface, they will be consumed at once in the reaction. Therefore, etching will more likely proceed along the direction where the fewest number of Si-Si bonds are needed to break,<sup>[23]</sup> like the family of  $\langle 100 \rangle$  crystalline directions. In the trenches shown in Figs. 2(a) and (b), the

**Fig. 3.** Schematic illustration of the formation of a slant sidewall trench.

‘grass-like’ nanowires can be related to the tendency of etching along the  $\langle 100 \rangle$  directions. Because of the thin layer of noble metal as the catalyst, the region of highest holes concentration is located right beneath the metal. The etching thus favors where noble metal existed, as illustrated in Fig. 3, resulting in an anisotropic etch and thus a vertical sidewall on the substrate.

#### 4. CONCLUSIONS

In this paper, we have demonstrated the use of MACE for the etching of trenches. A layer of 10 nm-thick interconnected Au islands was evaporated as the catalyst and the etchant of  $\text{HF}/\text{H}_2\text{O}_2$  mixture solution with different  $\rho$ 's was used in this experiment. Various tilting angles of the etched trenches on different resistivity Si substrates were observed. The relationship between the tilting angle of the trench sidewall and  $\rho$  of the etchant and the doping level of the substrates was proposed. Vertical trench was obtained on the 10  $\Omega \cdot \text{cm}$  silicon substrate by etching in a  $\rho(0.37)$  etchant with  $[\text{HF}] = 3.96 \text{ M}$ . This process has promising applications on many fields requiring high aspect ratio structures.

#### ACKNOWLEDGEMENTS

The authors thank the Center for Advanced Electronic Materials and Devices at Shanghai Jiao Tong University for SEM support. The authors acknowledge the financial support from the Shanghai Institute of Applied Physics, CAS and the Science and Technology Commission of Shanghai Municipality under Grant #13ZR1420700.

#### REFERENCES

1. D. Hernandez, D. Lange, T. Trifonov, M. Garín, M. García, A. Rodríguez, and R. Alcubilla, *Microelectron. Eng.* **87**, 1458 (2010).
2. M. D. Kelzenberg, S. W. Boettcher, J. A. Petykiewicz, D. B. Turner-Evans, M. C. Putnam, E. L. Warren, J. M. Spurgeon, R. M. Briggs, N. S. Lewis, and H. A. Atwater, *Nat.*

- Mater.* **9**, 239 (2010).
3. K. Q. Peng, X. Wang, L. Li, X. L. Wu, and S. T. Lee, *J. Am. Chem. Soc.* **132**, 6872 (2010).
  4. Y. Cui, Q. Wei, H. Park, and C. M. Lieber, *Science* **293**, 1289 (2001).
  5. B. R. Murthy, J. K. K. Ng, E. S. Selamat, N. Balasubramanian, and W. T. Liu, *Biosens. Bioelectron.* **24**, 723 (2008).
  6. K. Peng, J. Jie, W. Zhang, and S.-T. Lee, *Appl. Phys. Lett.* **93**, 033105 (2008).
  7. A. I. Hochbaum, R. Chen, R. D. Delgado, W. Liang, E. C. Garnett, M. Najarian, A. Majumdar, and P. Yang, *Nature* **451**, 163 (2008).
  8. A. Snigirev, I. Snigireva, M. Grigoriev, V. Yunkin, M. D. Michiel, G. Vaughan, V. Kohn, and S. Kuznetsov, *J. Phys.: Conf. Ser.* **186**, 012072 (2009).
  9. J. Bondur, *J. Vac. Sci. Technol.* **13**, 1023 (1976).
  10. M. Ahn, R. K. Heilmann, and M. L. Schattenburg, *J. Vac. Sci. Technol. B* **25**, 2593 (2007).
  11. V. Lehmann and H. Föll, *J. Electrochem. Soc.* **137**, 653 (1990).
  12. V. Lehmann and U. Grüning, *Thin Solid Films* **297**, 13 (1997).
  13. H. Föll, M. Christophersen, J. Carstensen, and G. Hasse, *Mater. Sci. Eng. R* **39**, 93 (2002).
  14. P. Lianto, S. Yu, J. Wu, C. V. Thompson, and W. K. Choi, *Nanoscale* **4**, 7532 (2012).
  15. L. Li, Y. Liu, X. Zhao, Z. Lin, and C. P. Wong, *ACS Appl. Mater. Inter.* **6**, 575 (2013).
  16. Z. Huang, N. Geyer, P. Werner, J. De Boor, and U. Gösele, *Adv. Mater.* **23**, 285 (2011).
  17. X. Li and P. W. Bohn, *Appl. Phys. Lett.* **77**, 2572 (2000).
  18. M. L. Zhang, K. Q. Peng, X. Fan, J. S. Jie, R. Q. Zhang, S. T. Lee, and N. B. Wong, *J. Phys. Chem. C* **112**, 4444 (2008).
  19. M. Lajvardi, H. Eshghi, M. Izadifard, M. E. Ghazi, and A. Goodarzi, *Physica E* **75**, 136 (2016).
  20. C. Y. Chen, Y. R. Liu, J. C. Tseng, and P. Y. Hsu, *Appl. Surf. Sci.* **333**, 152 (2015).
  21. S. Cruz, A. Hönig-d'Orville, and J. Müller, *J. Electrochem. Soc.* **152**, C418 (2005).
  22. J. Huang, S. Y. Chiam, H. H. Tan, S. Wang, and W. K. Chim, *Chem. Mater.* **22**, 4111 (2010).
  23. Z. Huang, T. Shimizu, S. Senz, Z. Zhang, N. Geyer, and U. Gösele, *J. Phys. Chem. C* **114**, 10683 (2010).